

Energy mode distribution: an analysis of the ratio of anti-Stokes to Stokes amplitudes generated by a pair of counterpropagating Langmuir waves.

Fernando J. R. Simões Júnior^{a*}, M. Virgínia Alves^a, Felipe B. Rizzato^b

^aInstituto Nacional de Pesquisas Espaciais, S. J. dos Campos, SP, Brazil

^bUniversidade Federal do Rio Grande do Sul, IF-UFRGS, Porto Alegre, RS, Brazil

Abstract

Results from plasma wave experiments in spacecraft give support to nonlinear interactions involving Langmuir, electromagnetic, and ion-acoustic waves in association with type III solar radio bursts. Starting from a general form of Zakharov equation (Zakharov, 1984), the equations for electric fields and density variations (density gratings) induced by a pair of counterpropagating Langmuir waves are obtained. We consider the coupling of four triplets. Each two triplets have in common the Langmuir pump wave (forward or backward wave) and a pair of independent density gratings. We solve numerically the dispersion relation for the system, extending the work of Alves et al.,(2002). The ratio of anti-Stokes (AS) ($\omega_0 + \omega$) to Stokes (S) ($\omega_0 - \omega^*$) electromagnetic mode amplitudes is obtained as a function of the pump wave frequency, wave number, and energy. We notice that the simultaneous excitation of AS and S distinguishable modes, i.e., with $Re\{\omega\} = \omega_r \neq 0$, only occurs for $r \neq 1$ and when $k_0 < (1/3)W_0^{1/2}$. We also observe that the S mode always receives more energy.

Keywords: *Plasma; Waves; Solar wind; Instabilities; Radio bursts.*

1 Introduction

In the last two decades, several models and theories related to type III solar radio bursts have been presented. The interplanetary type III radio bursts are a type of solar radio emission associated with energetic electron streams, accelerated either in solar flares or in active storm regions, that penetrate the solar corona and in-

*Corresponding author. Fax:+55 12 3945 6710

E-mail address: fernando@plasma.inpe.br

(Fernando Simões Jr.)

terplanetary medium, up to distances of 1 AU (Goldman, 1984; Lin et al., 1986). The electrons move away from the Sun and Langmuir waves are excited due to a beam-plasma instability. These Langmuir waves then interact with low-frequency fluctuation to generate fundamental radiation with frequencies near the local electron frequency due to a decay process which can be represented by $L \rightarrow L' + s$ where L is the Langmuir pump wave, L' is the Langmuir daughter wave and s is the ion-acoustic daughter wave. Analysis of threshold and maximum growth rate of this instability shows that the growth rate peaks when L' is backscattered relative to L (Robinson, 1997). In a forward step, the first wave can interact with the daughter waves to emit fundamental and harmonic radiation with frequencies near twice the local electron plasma frequency (Chian & Alves, 1988, Alves et al., 2002).

Lashmore-Davies (1974) was the first to show that the fundamental plasma emission ($\omega = \omega_{pe}$) could be the result of a nonlinear coupling of two wave triplets due counterpropagating Langmuir waves. Chian & Alves (1988), based on the idea of Lashmore-Davies (1974), formulate the theory for the case of two Langmuir pump waves and one mode of low frequency (grating - ion acoustic wave). Rizzato & Chian (1992) improved this model of two pump waves including a second grating (ion-acoustic wave) that assures the symmetry of the wave kinematics. Moreover, these authors investigated the simultaneous generation of electromagnetic and Langmuir daughter waves. Glanz et al. (1993) modified the model of Chian & Alves (1988) to allow for different amplitudes for the two Langmuir pump waves and included a second grating.

More recently, Alves et al. (2002) considered the emission of electromagnetic radiation generated by two counterpropagating pump waves with different amplitudes. These authors considered the presence of two gratings (ion-acoustic waves) and the generation of anti-Stokes ($\omega + \omega_0$) and Stokes ($\omega^* - \omega_0$) electromagnetic and Langmuir daughter waves. They obtained the general dispersion relation and solved it for two different values of k_0 , within the ranges: $k_0 > (2/3)(\mu\tau)^{1/2}$, where $\tau = (\gamma_e T_e + \gamma_i T_i)/T_e$, and $\mu = m_e/m_i$, and $k_0 < (1/3)W_0^{1/2}$, where W_0 is the pump wave energy. Those ranges were obtained considering the model of one pump wave; the resonant decay instability (three waves, $Re\{\omega\} = \omega_r = \omega_s$) occurs when $k_0 > (2/3)(\mu\tau)^{1/2}$; the purely growing instability ($\omega_r = 0$) occurs when $k_0 < (1/3)W_0^{1/2}$ (Akimoto 1988; Abalde et al. 1998). The general dispersion relation has been numerically solved using parameters relevant to type III solar radio bursts (Thejappa & MacDowall 1998).

Since electromagnetic waves can propagate only if they have frequencies larger than the plasma frequency, the observable excited mode would be the anti-Stokes mode ($\omega + \omega_0, \omega_r > 0$). Although our approach is valid

only for the onset of the instability, it is the aim of this paper to understand how the pump wave energy is distributed through the excited modes. We obtain the ratio of anti-Stokes (*AS*) to Stokes (*S*) electromagnetic mode amplitudes, R_{AS} , considering the model previously used by Alves et al., (2002). We solve the general dispersion relation obtained for Alves et al., (2002) for different cases; within the ranges where convective ($\omega_r \neq 0$) instability occurs, we obtain R_{AS} ; when the instability is purely growing, ($\omega_r = 0$), the *AS* and *S* modes are not distinguishable.

This paper is organized as follows: in Section 2 we present the fundamental equations used, derive the ratio of anti-Stokes to Stokes electromagnetic mode amplitudes, and present the dispersion relation. In Section 3 we discuss the numerical results obtained from solving the dispersion relation and use them to obtain R_{AS} . Conclusions are presented in Section 4.

2 Fundamental equations and energy mode distribution

The nonlinear coupling of Langmuir (*L*), electromagnetic (*T*) and ion-acoustic (*s*) waves is governed by the generalized Zakharov equations (Zakharov 1984; Akimoto 1988; Chian & Alves 1988; Rizzato & Chian 1992; Robinson 1997; Abalde et al. 1998; Bárta & Karlichy 2000)

$$(\partial_t^2 + \nu_e \partial_t + c^2 \nabla \times (\nabla \times) - \gamma_e v_{th}^2 \nabla (\nabla \cdot) + \omega_{pe}^2) \mathbf{E} = -\frac{\omega_{pe}^2}{n_0} n \mathbf{E}, \quad (1)$$

$$(\partial_t^2 + \nu_i \partial_t - v_s^2 \nabla^2) n = \frac{\varepsilon_0}{2m_i} \nabla^2 \langle \mathbf{E}^2 \rangle, \quad (2)$$

where \mathbf{E} is the high-frequency electric field, n is the ion density fluctuation, $\omega_{pe}^2 = n_0 e^2 / (m_e \varepsilon_0)$ is the electron plasma frequency, c is the velocity of light, $v_{th} = (k_B T_e / m_e)^{1/2}$ is the electron thermal velocity, $v_s = (k_B (\gamma_e T_e + \gamma_i T_i) / m_i)^{1/2}$ is the ion-acoustic velocity, $\nu_{e(i)}$ is the damping frequency for electrons (ions), $\gamma_{e(i)}$ is the ratio of the specific heats for electrons (ions), and the angle brackets denote the fast time average.

We assume that the electric field of the Langmuir pump waves is given by

$$\mathbf{E}_0 = \frac{1}{2} \left(\mathbf{E}_0^+ \exp[i(\mathbf{k}_0 \cdot \mathbf{r} - \omega_0 t)] + \mathbf{E}_0^- \exp[i(-\mathbf{k}_0 \cdot \mathbf{r} - \omega_0 t)] \right) + c.c., \quad (3)$$

which represents two pump waves counterpropagating of equal frequencies and opposite wave vectors. The amplitude of the pump waves can be different, $|\mathbf{E}_0^-|^2 = r |\mathbf{E}_0^+|^2$, with $0 \leq r \leq 1$. We consider that each pump wave can generate the anti-Stokes and Stokes electromagnetic and electrostatic waves, due a three wave process.

We consider the coupling of four triplets, assuming that each pair of triplets has in common the Langmuir pump

wave (forward or backward) and two independent density gratings, $n_{1(2)}$, given by

$$n = \frac{1}{2}n_{1(2)}\exp[i(\mathbf{k}_{1(2)} \cdot \mathbf{r} - \omega t)] + c.c.,$$

with $|\mathbf{k}_1| = |\mathbf{k}_2|$. The electromagnetic field for each one of the daughter waves is given by

$$\mathbf{E} = \frac{1}{2}\mathbf{E}_w^{+(-)}\exp[i(\mathbf{k}_w^{+(-)} \cdot \mathbf{r} - \omega_w^{+(-)}t)] + c.c., \quad (4)$$

where the subscript w represents either electromagnetic (T) or electrostatic (L) daughter wave; the superscript $+(-)$ represents the anti-Stokes (Stokes) mode. Fig. 1 illustrates the matching conditions for wave-vectors. The kinematic model implies that the two Langmuir pump waves propagate oppositely along the longitudinal x -axis, generating two opposite induced electromagnetic modes that primarily propagate along transverse y -axis, plus induced Langmuir modes that mainly propagate along the x -axis. This chosen kinematic is based on the fact that the coupling between pump and electromagnetic waves is more efficient when the electric fields have the same directions (Glanz et al., 1993).

The linear dispersion relations for the waves considered in the our model are given by

$$\begin{aligned} \mathcal{D}_{S1(2)} &= \omega^2 + i\nu_s\omega - v_s^2k_{1(2)}^2, \\ \mathcal{D}_T^\pm &= [(\omega_0 \pm \omega)^2 + i\nu_T(\omega_0 \pm \omega) - c^2k_T^{\pm 2} - \omega_p^2], \\ \mathcal{D}_{L1(2)}^\pm &= [(\omega_0 \pm \omega)^2 + i\nu_L(\omega_0 \pm \omega) - v_{th}^2k_{L1(2)}^{\pm 2} - \omega_p^2], \end{aligned} \quad (5)$$

where $\mathcal{D}_{S1(2)}$ stands for the ion-acoustic wave, \mathcal{D}_T^\pm for the electromagnetic daughter wave, $\mathcal{D}_{L1(2)}^\pm$ for the Langmuir daughter wave, and $\nu_w, w = s, T,$ and L represents the damping wave frequencies. Observe that we assume $|\mathbf{k}_{L1}^\pm| \simeq |\mathbf{k}_{L2}^\pm|$, and $|\mathbf{k}_T^+| \simeq |\mathbf{k}_T^-|$, as shown in Fig. 1. Also, the adopted geometry implies in $|k_T^\pm| \ll |k_0|, |k_{L1(2)}^\pm|, |k_{1(2)}|$.

In order to obtain the equation that relates the anti-Stokes to the Stokes mode, we write the total high frequency fluctuating fields in terms of its transverse and longitudinal component, $\mathbf{E} = \mathbf{E}_l + \mathbf{E}_t$, imposing perfect \mathbf{k} -matching but allowing for frequency mismatches between the interacting waves. Using the kinematic conditions

presented in Fig. 1 in Eq. (1), we can describe the induced wave variations as follows

$$\mathcal{D}_{L1}^- E_{L1}^- = \frac{\omega_p^2}{n_0} n_1^* E_0^-, \quad (6)$$

$$\mathcal{D}_{L1}^+ E_{L1}^+ = \frac{\omega_p^2}{n_0} n_1 E_0^+, \quad (7)$$

$$\mathcal{D}_{L2}^- E_{L2}^- = \frac{\omega_p^2}{n_0} n_2^* E_0^+, \quad (8)$$

$$\mathcal{D}_{L2}^+ E_{L2}^+ = \frac{\omega_p^2}{n_0} n_2 E_0^-, \quad (9)$$

$$\mathcal{D}_T^+ E_T^+ = \frac{\omega_p^2}{n_0} (n_1 E_0^- + n_2 E_0^+), \quad (10)$$

$$\mathcal{D}_T^- E_T^- = \frac{\omega_p^2}{n_0} (n_1^* E_0^+ + n_2^* E_0^-). \quad (11)$$

In Eqs. (6-11) the sub-index $L_{1(2)}$ refers to Langmuir wave daughter due to first (second) grating.

Introducing Eqs. (6-11) in Eq. (2), we obtain the following equations for the density fluctuations

$$\mathcal{D}_{S1} n_1 = \frac{\varepsilon_0 k_1^2}{2m_i} [E_0^+ E_T^{-*} + E_0^- E_{L1}^{-*} + E_{L1}^+ E_0^{+*} + E_T^+ E_0^{-*}], \quad \text{and} \quad (12)$$

$$\mathcal{D}_{S2} n_2 = \frac{\varepsilon_0 k_2^2}{2m_i} [E_0^+ E_{L2}^{-*} + E_0^- E_T^{-*} + E_{L2}^+ E_0^{-*} + E_T^+ E_0^{+*}]. \quad (13)$$

Introducing Eqs. (6-9) into Eqs. (12-13), we obtain for n_1 and n_2

$$n_1 = \frac{\frac{\varepsilon_0 k_1^2}{2m_i}}{\mathcal{D}_{S1} - \frac{\varepsilon_0 k_1^2}{2n_0 m_i} \omega_{pe}^2 \left(\frac{E_0^- E_0^{-*}}{\mathcal{D}_{L1}^-} + \frac{E_0^+ E_0^{+*}}{\mathcal{D}_{L1}^+} \right)} [E_0^+ E_T^{-*} + E_T^+ E_0^{-*}], \quad (14)$$

$$n_2 = \frac{\frac{\varepsilon_0 k_2^2}{2m_i}}{\mathcal{D}_{S2} - \frac{\varepsilon_0 k_2^2}{2n_0 m_i} \omega_{pe}^2 \left(\frac{E_0^+ E_0^{+*}}{\mathcal{D}_{L2}^-} + \frac{E_0^- E_0^{-*}}{\mathcal{D}_{L2}^+} \right)} [E_0^- E_T^{-*} + E_T^+ E_0^{+*}]. \quad (15)$$

Introducing the equations for n_1 , n_2 , n_1^* and n_2^* into Eqs. (10) and (11), we obtain

$$\begin{aligned} \mathcal{D}_T^+ E_T^+ &= \frac{\omega_p^2}{n_0} \left(\frac{\frac{\varepsilon_0 k_1^2}{2m_i}}{\mathcal{D}_{S1} - \frac{\varepsilon_0 k_1^2}{2n_0 m_i} \omega_{pe}^2 \left(\frac{E_0^- E_0^{-*}}{\mathcal{D}_{L1}^-} + \frac{E_0^+ E_0^{+*}}{\mathcal{D}_{L1}^+} \right)} [E_0^+ E_T^{-*} + E_T^+ E_0^{-*}] E_0^- \right. \\ &\quad \left. + \frac{\frac{\varepsilon_0 k_2^2}{2m_i}}{\mathcal{D}_{S2} - \frac{\varepsilon_0 k_2^2}{2n_0 m_i} \omega_{pe}^2 \left(\frac{E_0^+ E_0^{+*}}{\mathcal{D}_{L2}^-} + \frac{E_0^- E_0^{-*}}{\mathcal{D}_{L2}^+} \right)} [E_0^- E_T^{-*} + E_T^+ E_0^{+*}] E_0^+ \right). \end{aligned} \quad (16)$$

In our approach we do not include the wave damping, i.e., we consider $\nu_w = 0$, ($w = s, L, T$). As a consequence,

we can assume that $\mathcal{D}_T^+ = \mathcal{D}_T^{+*}$, $\mathcal{D}_T^- = \mathcal{D}_T^{-*}$, $\mathcal{D}_L^+ = \mathcal{D}_L^{+*}$, $\mathcal{D}_L^- = \mathcal{D}_L^{-*}$ e $\mathcal{D}_S = \mathcal{D}_S^*$. Due to the kinematic

model adopted (Fig. 1) $|k_1| \simeq |k_2| = k$, and we can write Eq. (16) as

$$\begin{aligned}
& \left(\mathcal{D}_T^+ - \frac{\frac{\mathcal{D}_L^- \mathcal{D}_L^+ k^2 |E_0^+|^2 \omega_{pe}^2 \varepsilon_0}{2m_i}}{\mathcal{D}_L^- \mathcal{D}_L^+ \mathcal{D}_S n_0 - \frac{\mathcal{D}_L^+ k^2 |E_0^+|^2 \omega_{pe}^2 \varepsilon_0}{2m_i} - \frac{r \mathcal{D}_L^- k^2 |E_0^+|^2 \omega_{pe}^2 \varepsilon_0}{2m_i}} \right. \\
& \quad \left. - \frac{\frac{r \mathcal{D}_L^- \mathcal{D}_L^+ k^2 |E_0^+|^2 \omega_{pe}^2 \varepsilon_0}{2m_i}}{\mathcal{D}_L^- \mathcal{D}_L^+ \mathcal{D}_S n_0 - \frac{\mathcal{D}_L^- k^2 |E_0^+|^2 \omega_{pe}^2 \varepsilon_0}{2m_i} - \frac{r \mathcal{D}_L^+ k^2 |E_0^+|^2 \omega_{pe}^2 \varepsilon_0}{2m_i}} \right) E_T^+ \\
& = \left(\frac{\frac{\mathcal{D}_L^- \mathcal{D}_L^+ k^2 E_0^+ E_0^- \omega_{pe}^2 \varepsilon_0}{2m_i}}{\mathcal{D}_L^- \mathcal{D}_L^+ \mathcal{D}_S n_0 - \frac{\mathcal{D}_L^+ k^2 |E_0^+|^2 \omega_{pe}^2 \varepsilon_0}{2m_i} - \frac{r \mathcal{D}_L^- k^2 |E_0^+|^2 \omega_{pe}^2 \varepsilon_0}{2m_i}} \right. \\
& \quad \left. + \frac{\frac{\mathcal{D}_L^- \mathcal{D}_L^+ k^2 E_0^+ E_0^- \omega_{pe}^2 \varepsilon_0}{2m_i}}{\mathcal{D}_L^- \mathcal{D}_L^+ \mathcal{D}_S n_0 - \frac{\mathcal{D}_L^- k^2 |E_0^+|^2 \omega_{pe}^2 \varepsilon_0}{2m_i} - \frac{r \mathcal{D}_L^+ k^2 |E_0^+|^2 \omega_{pe}^2 \varepsilon_0}{2m_i}} \right) E_T^{-*}. \tag{17}
\end{aligned}$$

Defining $\mathcal{G}(\omega, k_T)$ and $\mathcal{F}(\omega, k_T)$ as

$$\begin{aligned}
\mathcal{G}(\omega, k_T) = \mathcal{D}_T^+ - \frac{\frac{\mathcal{D}_L^- \mathcal{D}_L^+ k^2 |E_0^+|^2 \omega_{pe}^2 \varepsilon_0}{2m_i}}{\mathcal{D}_L^- \mathcal{D}_L^+ \mathcal{D}_S n_0 - \frac{\mathcal{D}_L^+ k^2 |E_0^+|^2 \omega_{pe}^2 \varepsilon_0}{2m_i} - \frac{r \mathcal{D}_L^- k^2 |E_0^+|^2 \omega_{pe}^2 \varepsilon_0}{2m_i}} \\
- \frac{\frac{r \mathcal{D}_L^- \mathcal{D}_L^+ k^2 |E_0^+|^2 \omega_{pe}^2 \varepsilon_0}{2m_i}}{\mathcal{D}_L^- \mathcal{D}_L^+ \mathcal{D}_S n_0 - \frac{\mathcal{D}_L^- k^2 |E_0^+|^2 \omega_{pe}^2 \varepsilon_0}{2m_i} - \frac{r \mathcal{D}_L^+ k^2 |E_0^+|^2 \omega_{pe}^2 \varepsilon_0}{2m_i}}, \tag{18}
\end{aligned}$$

$$\begin{aligned}
\mathcal{F}(\omega, k_T) = \frac{\frac{\mathcal{D}_L^- \mathcal{D}_L^+ k^2 E_0^+ E_0^- \omega_{pe}^2 \varepsilon_0}{2m_i}}{\mathcal{D}_L^- \mathcal{D}_L^+ \mathcal{D}_S n_0 - \frac{\mathcal{D}_L^+ k^2 |E_0^+|^2 \omega_{pe}^2 \varepsilon_0}{2m_i} - \frac{r \mathcal{D}_L^- k^2 |E_0^+|^2 \omega_{pe}^2 \varepsilon_0}{2m_i}} \\
+ \frac{\frac{\mathcal{D}_L^- \mathcal{D}_L^+ k^2 E_0^+ E_0^- \omega_{pe}^2 \varepsilon_0}{2m_i}}{\mathcal{D}_L^- \mathcal{D}_L^+ \mathcal{D}_S n_0 - \frac{\mathcal{D}_L^- k^2 |E_0^+|^2 \omega_{pe}^2 \varepsilon_0}{2m_i} - \frac{r \mathcal{D}_L^+ k^2 |E_0^+|^2 \omega_{pe}^2 \varepsilon_0}{2m_i}}, \tag{19}
\end{aligned}$$

we can write Eq. (17) in a shorter form

$$\mathcal{G}(\omega, k_T) E_T^+ = \mathcal{F}(\omega, k_T) E_T^{-*}. \tag{20}$$

Using the high-frequency approximation we can write that $\mathcal{D}_T^\pm \cong \pm 2\omega_p(\omega \pm (\omega_0 - \omega_T))$, $\mathcal{D}_{L1(2)}^\pm \cong \pm 2\omega_p(\omega \pm (\omega_0 - \omega_L))$, where $\omega_{L(T)}$ represents the linear dispersion relation of the Langmuir (electromagnetic) wave. In order to have a better numerical treatment, we normalize all variables as follows: ω by ω_s and k, k_0 , and k_T by $1/\lambda_D$ where λ_D is the electron Debye length. As a result, Eqs. (5) normalized are,

$$\begin{aligned}
D_S &= \omega^2 - 1 \\
D_T^\pm &= \omega \pm \frac{3}{2} \frac{k_0}{(\mu\tau)^{1/2}} \mp \frac{1}{2} \frac{c^2}{v_{th}^2} \frac{k_T^2}{(\mu\tau)^{1/2} k_0} \\
D_L^\pm &= \omega \mp \frac{9}{2} \frac{k_0}{(\mu\tau)^{1/2}}. \tag{21}
\end{aligned}$$

Finally, recalling that $|\mathbf{E}_0^-|^2 = r|\mathbf{E}_0^+|^2$, and defining $W_0 = \varepsilon_0 |\mathbf{E}_0^+|^2 / (2n_0 k_B T_e)$, and $W_{T0} = (1+r)W_0$, we obtain

the following normalized equation for $\mathcal{G}(\omega, k_T)$ and $\mathcal{F}(\omega, k_T)$

$$|G(\omega, k_T)| = \left| D_T^+ - \frac{W_{T0}}{\tau^2 \mu k_0^2 (1+r)} \left(\frac{D_L^- D_L^+}{D_L^+ D_L^- D_S - \frac{D_L^+ W_{T0}}{\tau^2 \mu k_0^2 (1+r)} - \frac{r D_L^- W_{T0}}{\tau^2 \mu k_0^2 (1+r)}} - \frac{r D_L^- D_L^+}{D_L^+ D_L^- D_S - \frac{D_L^- W_{T0}}{\tau^2 \mu k_0^2 (1+r)} - \frac{r D_L^+ W_{T0}}{\tau^2 \mu k_0^2 (1+r)}} \right) \right|, \quad (22)$$

$$|F(\omega, k_T)| = \frac{r^{1/2} W_{T0}}{\tau^2 \mu k_0^2 (1+r)} \left| \left(\frac{D_L^- D_L^+}{D_L^+ D_L^- D_S - \frac{D_L^+ W_{T0}}{\tau^2 \mu k_0^2 (1+r)} - \frac{r D_L^- W_{T0}}{\tau^2 \mu k_0^2 (1+r)}} + \frac{D_L^- D_L^+}{D_L^+ D_L^- D_S - \frac{D_L^- W_{T0}}{\tau^2 \mu k_0^2 (1+r)} - \frac{r D_L^+ W_{T0}}{\tau^2 \mu k_0^2 (1+r)}} \right) \right|. \quad (23)$$

For the sake of simplicity we use the same symbols for wave number and frequency as we were using before normalization was done. The ratio of anti-Stokes to Stokes modes is then obtained introducing Eqs. (22) and (23) into Eq. (20) as

$$\left| \frac{E_T^+}{E_T^{*-}} \right| = \frac{\frac{r^{1/2} W_{T0}}{\tau^2 \mu k_0^2 (1+r)} \left| \left(\frac{D_L^- D_L^+}{D_L^+ D_L^- D_S - \frac{D_L^+ W_{T0}}{\tau^2 \mu k_0^2 (1+r)} - \frac{r D_L^- W_{T0}}{\tau^2 \mu k_0^2 (1+r)}} + \frac{D_L^- D_L^+}{D_L^+ D_L^- D_S - \frac{D_L^- W_{T0}}{\tau^2 \mu k_0^2 (1+r)} - \frac{r D_L^+ W_{T0}}{\tau^2 \mu k_0^2 (1+r)}} \right) \right|}{\left| D_T^+ - \frac{W_{T0}}{\tau^2 \mu k_0^2 (1+r)} \left(\frac{D_L^- D_L^+}{D_L^+ D_L^- D_S - \frac{D_L^+ W_{T0}}{\tau^2 \mu k_0^2 (1+r)} - \frac{r D_L^- W_{T0}}{\tau^2 \mu k_0^2 (1+r)}} - \frac{r D_L^- D_L^+}{D_L^+ D_L^- D_S - \frac{D_L^- W_{T0}}{\tau^2 \mu k_0^2 (1+r)} - \frac{r D_L^+ W_{T0}}{\tau^2 \mu k_0^2 (1+r)}} \right) \right|}. \quad (24)$$

The dispersion relation that describes the wave coupling represented in Fig. 1, as presented by Alves et al., (2002), can be obtained using Eqs. (12-13), with all definitions and approximations introduced in this paper.

The general dispersion relation is given by

$$\begin{aligned} D_S^2 - \frac{W_{T0}}{4\tau(\mu\tau)^{1/2}k_0} D_S \left(\frac{1}{D_L^+} - \frac{1}{D_L^-} + \frac{1}{D_T^+} - \frac{1}{D_T^-} \right) + \frac{W_{T0}^2}{16\mu\tau^3 k_0^2 (1+r)^2} \left[\frac{-(1-r)^2}{D_T^+ D_T^-} \right. \\ \left. + (1+r^2) \left(\frac{1}{D_T^+ D_L^+} - \frac{1}{D_L^+ D_L^-} + \frac{1}{D_T^- D_L^-} \right) - 2r \left(\frac{1}{D_L^+ D_T^-} + \frac{1}{D_T^+ D_L^-} \right) \right. \\ \left. + r \left(\frac{1}{D_L^{+2}} + \frac{1}{D_L^{-2}} \right) \right] = 0, \end{aligned} \quad (25)$$

where, D_S , D_L and D_T are the same of Eq. (21).

Alves et al. (2002) have shown that the dispersion relation, with the suitable approximation, includes several models found in the literature (Akimoto, 1988; Abalde et al., 1998; Rizzato & Chian, 1992; Chian & Alves, 1988; Glanz et al., 1993). They have also shown that when $k_0 < (1/3)W_0^{1/2}$, the presence of a second pump wave, with different amplitude from the first one ($r \neq 1$), introduces a region of convective, nonresonant instability ($\omega_r \neq 0$, $\omega_r \neq \omega_S$), not present when $r = 1$.

In this paper we numerically solve the general dispersion relation (Eq. (25)) to establish the range where instability occurs and when the anti-Stokes and Stokes distinguishable modes, i.e., with $Re\{\omega\} = \omega_r \neq 0$ (convective

instability), are simultaneously excited. The ratio of anti-Stokes to Stokes electromagnetic mode amplitudes, R_{AS} , is then calculated only when the instability is convective. For purely growing instability ($\omega_r = 0$) the anti-Stokes and Stokes modes are indistinguishable.

3 Numerical solution

A one pump wave model predicts the instability to behave differently within the two following ranges: for $k_0 > (2/3)(\mu\tau)^{1/2}$, where $\tau = (\gamma_e T_e + \gamma_i T_i)/T_e$, and $\mu = m_e/m_i$, a resonant decay instability (three waves, $\omega_r = \omega_s$) occurs. When $k_0 < (1/3)W_0^{1/2}$, where W_0 is the energy of the pump wave, a purely growing instability ($\omega_r = 0$) occurs. Although the *AS* and *S* modes are simultaneously excited in the last case, they are not distinguishable. For our model, considering two pump waves with different amplitudes, a similar limit exists. Moreover, when $k_0 < (1/3)W_0^{1/2}$, $r \neq 1$, $r \neq 0$, a convective ($\omega_r \neq 0$) instability occurs for some ranges of k_T (Alves et al., 2002), and anti-Stokes and Stokes distinguishable modes are simultaneously excited. In that sense, all results presented in this section will be within the range $k_0 < (1/3)W_0^{1/2}$.

In order to obtain the numerical solution of the general dispersion relation, we consider parameters relevant to type III solar radio bursts (Thejappa & MacDowall 1998). We use a fixed value of $\mu = 1/1836$, $v_{th} = 2.2 \times 10^6 m/s$, $T_e = 1.6 \times 10^5 K$, $T_i = 5 \times 10^4 K$, $\tau = 1.520$, and $k_0 = 10^{-4}$.

Fig. 2 shows the numerical results of the general dispersion relation as a function of r and k_T . Fig.2-(a) represents the real part of the frequency (ω_r) and Fig. 2-(b) represents the growth rate (Γ). We notice three different regions of instability: for k_T less than 10^{-5} , instability is purely growing ($\omega_r = 0$), independent of the value of r ; for k_T larger than 10^{-5} the instability is non-resonant and convective ($\omega_r \neq \omega_s$, $\omega_r \neq 0$) except for a small region, found approximately at $k_T > 3 \times 10^{-5}$ and r between 0.4 and 0.7, when $\Gamma = 0$. As r increases, the range of k_T where non-resonant and convective instability occurs decreases. For $r = 1$, only purely growing instability occurs, independent of the values of k_T .

In order to obtain R_{AS} , first we solve the dispersion relation as a function of the total energy of the system W_{T0} and the wave number of electromagnetic wave k_T , for a fixed value of $r = 0.5$ and of $k_0 = 10^{-4}$. Fig. 3 shows the numerical solution for this case. Fig. 3-(a) represents the real part of the frequency ω_r and Fig. 3-(b) represents the growth rate Γ . For a given W_{T0} , we find the range of k_T where the instability is convective ($\omega_r \neq 0$) and find the corresponding k_T which gives the maximum growth rate. Fig. 4 presents the results for R_{AS} as a function of W_{T0} , calculated for the value k_T which gives the maximum Γ and corresponding frequency.

Although we do not show, the values of k_T that give the maximum Γ are within the range 1.2×10^{-5} and 2.5×10^{-5} , compatible with results presented in Fig. 2. Since $R_{AS} < 1$, for this particular case, the Stokes mode receives more energy. Similar results are obtained for different values of $r \neq 1$.

4 Conclusion

In this paper we have presented the formalism to obtain the ratio of the anti-Stokes to Stokes mode energy amplitude, starting from the Zakharov equations with a model that considers two counterpropagating Langmuir pump waves with different amplitudes.

From numerical analysis of the general dispersion relation we notice that depending on the ratio of the Langmuir pump wave amplitudes, r , we have ranges of k_T where convective or purely growing instability occurs and also regions of no instability, as shown in Fig. 1.

Using a fixed value for $r \neq 1$ we observe the simultaneous excitation of anti-Stokes and Stokes distinguishable modes (convective, no resonant instability (see Fig. 2)). Although we present results just for $r = 0.5$, similar results have been obtained for different parameters. In general, the Stokes mode receives more energy.

In a future work, we should include the wave damping rates. By comparing the wave damping rates with the instability growth rate we can verify the efficiency of the process for emission of electromagnetic waves.

Acknowledgments: We would like to thank Dr. Abraham C.-L. Chian for useful discussion. This work has been partially supported by Conselho Nacional de Desenvolvimento Científico e Tecnológico (CNPq - Brasil).

References

- Alves, M. V., Chian, A. C. L., Moraes, M. A. E., Abalde, J. R., Rizzato, F. B., 2002. A theory of the fundamental plasma emission of type- III solar radio bursts. *Astronomy and Astrophysics*, 390: 351-357.
- Abalde J. R., Alves, M. V., Chian, A. C. L., 1998. Nonlinear generation of type III solar radio bursts by the hybrid modulational instability. *Astronomy and Astrophysics*. 331, L21-L24.
- Akimoto, K., 1988. Electromagnetic effects on parametric instabilities of Langmuir waves. *Physics of Fluids*. 31(3): 538-546.
- Bárta, M., Karlický, M., 2000. Energy mode distribution at the very beginning of parametric instabilities of monochromatic Langmuir waves. *Astronomy and Astrophysics*. 353, 757-770.
- Chian, A. C. L., Alves, M. V., 1988. Nonlinear generation of the fundamental radiation of interplanetary type

III radio bursts. *The Astrophysical Journal*. 330(1): L77-L80.

Glanz, J., Goldman, M. V., Newman, D. L., 1993. Electromagnetic instability and emission from counterpropagating Langmuir waves. *Physics of Fluids*. B5(4).

Goldman, M. V., 1984. Strong turbulence of plasma waves. *Reviews of Modern Physics*. 56(4): 709-735.

Lin, R. P., Levedahl, W. K., Lotko W., Gurnett D. A., Scarf F. L., 1986. Evidence for nonlinear wave-wave interaction in solar type III radio bursts. *The Astrophysical Journal*. 308: 954-965.

Lashmore-Davies, C. N., 1974. Parametric up-conversion of Langmuir into transverse electromagnetic waves. *Physics Reviews Letters*. 32(6): 289-291.

Rizzato, F. B., Chian, A. C. L., 1992. Nonlinear generation of the fundamental radiation in plasmas: the influence of induced ion-acoustic and Langmuir waves. *Journal of Plasma Physics*. 48(1): 71-84.

Robinson, P. A., 1997. Nonlinear wave collapse and strong turbulence. *Reviews of Modern Physics*. 69(2), 507-573.

Thejappa, G., MacDowall, R. J., 1998. Evidence for strong turbulence process in the region of a local type III radio bursts. *The Astrophysical Journal*. 498: 465-478.

Zakharov, V. E., 1985. Collapse and self-focusing of Langmuir waves. *Handbook of Plasma Physics*. Cap.2, 81-121.

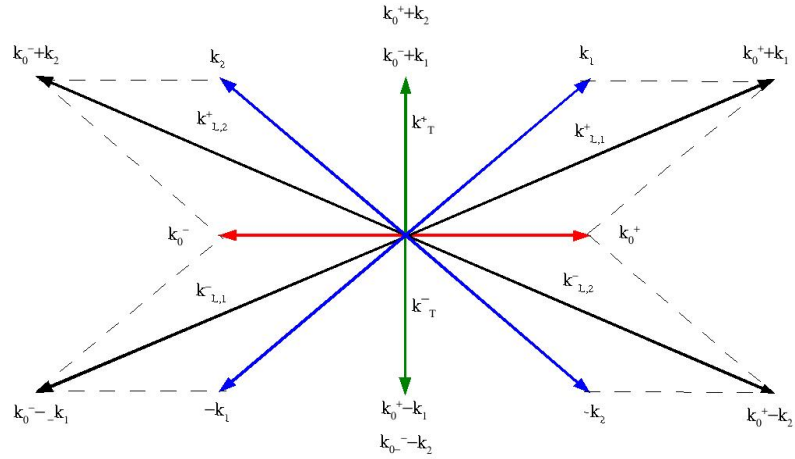
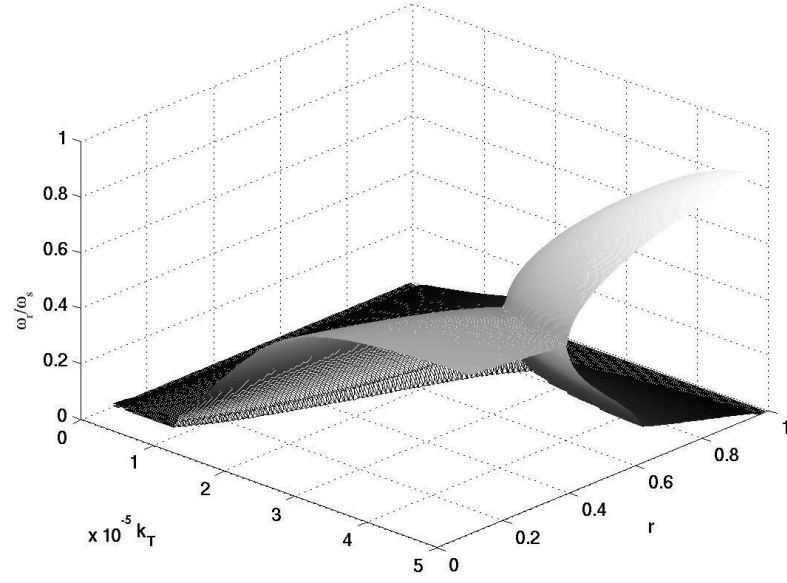
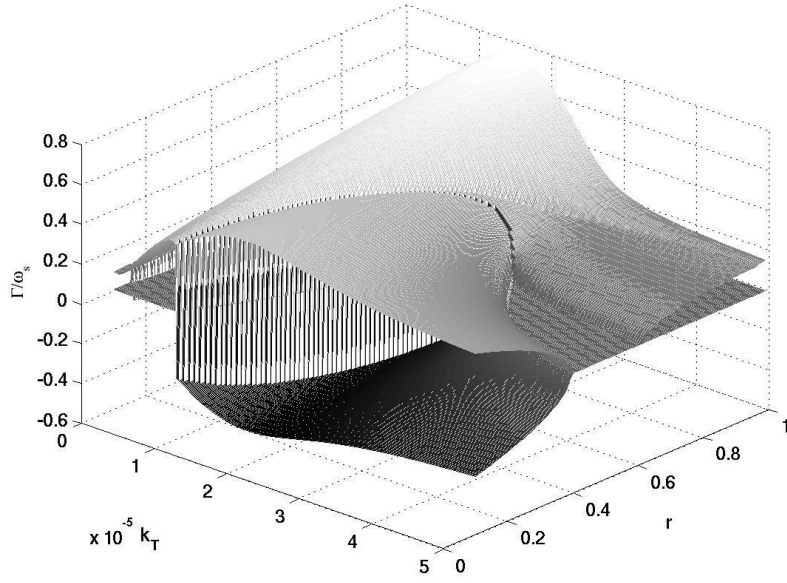


Figure 1: Wave-vector kinematics for our model: $k_0^{-(+)}$ are related to the pump Langmuir waves, $k_{1(2)}$ to ion acoustic waves, $(k_0^{+(-)} - k_{1(2)})$ are the electrostatic (oblique to $k_0^{+(-)}$) or electromagnetic (\perp a $k_0^{+(-)}$) Stokes modes and $(k_0^{+(-)} + k_{1(2)})$ are the electrostatic (oblique to $k_0^{+(-)}$) or electromagnetic (\perp a $k_0^{+(-)}$) anti-Stokes modes.

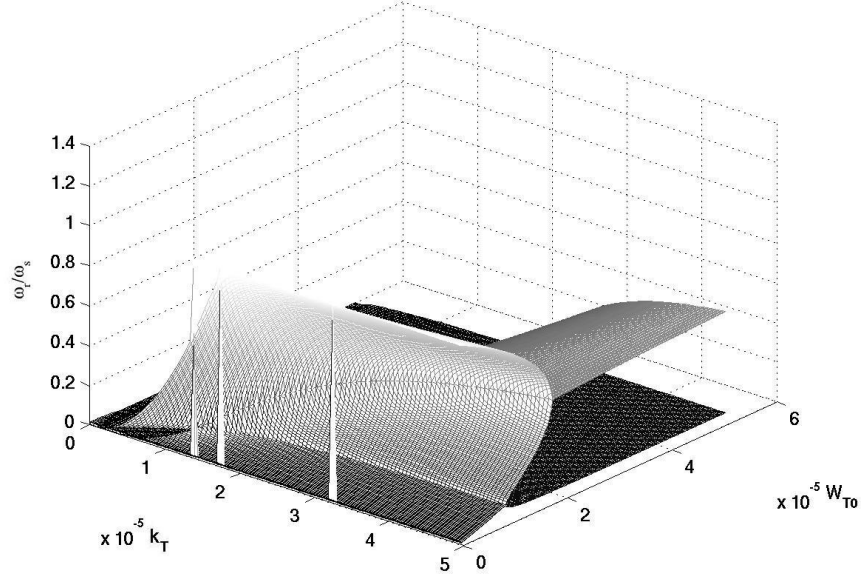


(a) Real frequency.

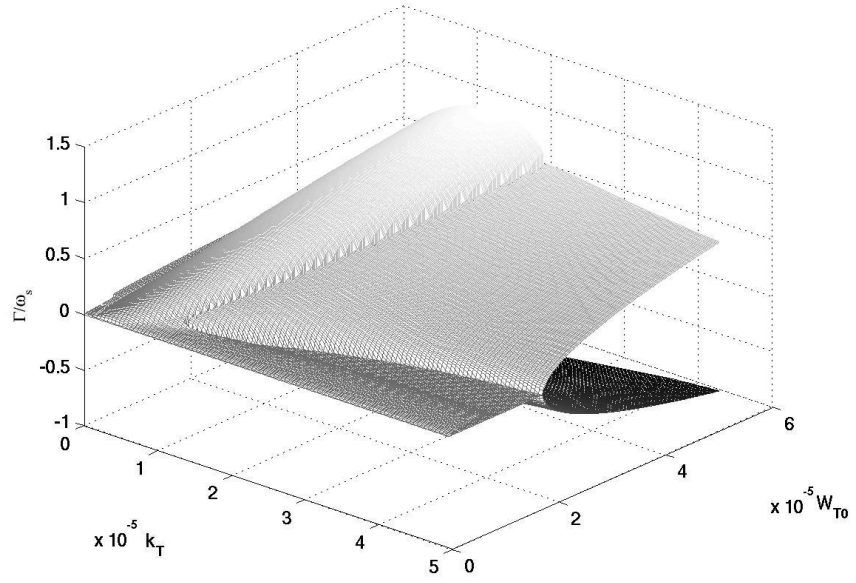


(b) Growth rate.

Figure 2: Numerical solution of the general dispersion relation as a function of r and k_T , with $k_0 = 10^{-4}$, within the limit $k_0 < (1/3)W_0^{1/2}$.



(a) Real frequency.



(b) Growth rate.

Figure 3: Numerical solution of the general dispersion relation as a function of W_{T0} and k_T , with $r = 0.5$, $k_0 = 10^{-4}$, within the limit $k_0 < (1/3)W_0^{1/2}$.

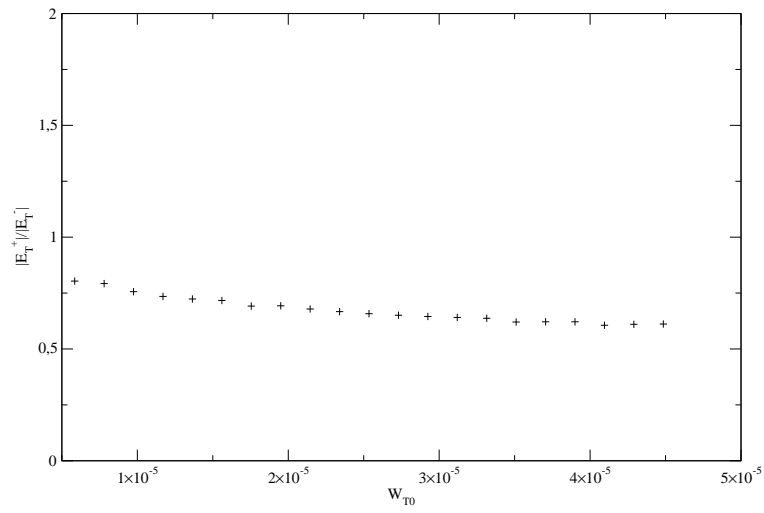


Figure 4: Ratio of anti-Stokes to Stokes mode amplitudes as a function of W_{T0} , for the same parameters as in Fig. 3, calculated for k_T which gives the maximum value of Γ .